J. Comp. App. Res. Mech. Eng. Vol. 13. No. 2, pp. 219-228, 2024 *DOI:10.22061/JCARME.2024.10109.2353*

Journal of Computational and Applied Research in Mechanical Engineering

jcarme.sru.ac.ir

SRTTU

JCARME

ISSN: 2228-7922

Research paper

Comparison of the performance of mesh and simple baffles in controlling the sloshing phenomenon based on the SPH simulation

R. Shamsoddini [a,*] and B. Abolpour [b]

[a]*Department of Mechanical Engineering, Sirjan University of Technology, Sirjan, Kerman, 7813733385, Iran*
[b]*Department of Chemical Engineering, Sirjan University of Technology, Sirjan, Kerman,7813733385, Iran*

Article info:

Article history:

Received: 06/08/2023
Revised: 17/01/2024
Accepted: 20/01/2024
Online: 22/01/2024

Keywords:
Simple baffle,
Mesh baffle,
SPH,
Hydrodynamic forces,
Sloshing.

***Corresponding author:**
shamsoddini@sirjantech.ac.ir

Abstract

One of the main problems in liquid transfer tanks is the sloshing phenomenon. This phenomenon, which is associated with regular or irregular liquid waves inside the tank, can cause many risks. One of the most widely applied methods to control the fluctuations caused by the sloshing phenomenon is the use of baffles. Baffles are usually installed vertically or horizontally on the inner wall of the tank. In uniform samples (simple baffle), the hydrodynamic force on the baffle is significant. Therefore, in this research, mesh baffle from the category of permeable baffles is introduced and tested, which can significantly reduce the hydrodynamic forces on the baffle. Therefore, in the present work, the sloshing phenomenon in a rectangular tank is first modeled by smoothed particle hydrodynamics and validated. Then, the tank with a simple baffle and mesh baffle are modeled and examined. During the numerical solution (in each time interval), the hydrodynamic forces acting on the baffles are monitored and extracted. The comparison of the obtained results shows that in addition to reducing the fluctuations of the sloshing phenomenon, the mesh baffle also creates a lower hydrodynamic resistance force.

1. Introduction

The sloshing phenomenon is the dominant phenomenon in fluid-carrying tanks. This phenomenon can be seen in LNG ships, tankers, and oil truck carriers. The motion of the solid body is transferred to the fluid, creating a turbulent movement of the fluid inside the tank, which is often associated with the formation of regular or irregular waves. These waves can sometimes introduce huge forces into the body of the tank, which causes many risks for the vehicle. Therefore, the control of these waves has always been considered one of the biggest refinements in this field. Due to the importance of the subject, many researchers have studied, examined, and provided solutions to reduce the fluctuations caused by the sloshing phenomenon, a few of which are mentioned below.

One of the leading studies in this field is the work of Modi and Munshi [1], who presented a damper to control the fluctuations caused by liquid slathering. The results showed that the

optimal damper can have a 60% effect. Kim *et al.* [2] considered the coupling effects of sloshing and ship motion. They observed that the motion of the ship is strongly sensitive to the slope of the wave. Brizzolara *et al.* [3] compared the numerical and experimental sloshing loads in partly filled tanks. Their results showed the appropriate relative accuracy of the smoothed particle hydrodynamics (SPH) method compared to other numerical methods. Xue and Lin [4] studied the effects of ring baffle on the decreasing violent liquid sloshing.

Molin and Remy [5] studied the sloshing phenomenon in a tank with a perforated screen numerically and experimentally. They found damping factors to be large over a wide range of frequencies, including the frequencies of the first two sloshing. Hosseinzadeh *et al.* [6] studied the shake table of annular baffles in storage tanks as the dependent variable of sloshing dampers. They reported that the added baffles do not considerably alter the impulsive and convective mode frequencies of the investigated tank model. Lu *et al.* [7] presented a two-dimensional simulation of viscous liquid sloshing in a rectangular tank with/without baffles and compared its results with potential flow solution results. They stated that both methods produce nearly identical solutions at the initial stage. Cho and Kim [8] studied the effects of dual porous vertical baffles on the reduction of sloshing in a swaying rectangular tank. They observed that the sloshing force and pressure on the wall are connected to the variation of the wall amplification factor. Xue *et al.* [9] studied the effects of vertical baffles of different shapes in restraining sloshing pressure experimentally.

Based on their results, the vertical baffle flushing with a free surface and the vertical perforated baffle are two more effective devices in decreasing the dynamic impact pressure. Kim *et al.* [10] investigated the induced pressure of sloshing in various scale tanks. They observed that the maximum sloshing pressures did not happen at the same position although the tank motion was harmonic. Wang *et al.* [11] investigated the liquid fill levels and effects of the length and arrangement of various baffles on the frequencies and modes of sloshing. One of their main results is that "the effect of baffles on the slosh frequencies is much smaller for excitation in the longitudinal direction than for excitation in the horizontal direction."

Wang and Sun [12] studied the liquid sloshing features in a tank with a baffle fixed vertically at the bottom of the tank. They investigated liquid sloshing features with an analytical solution based on the theory of linear velocity potential. Through their adjustment, wave removal can be obtained whether the sway motion frequency is near to or far away from the resonant frequency. Guan *et al.* [13] simulated the sloshing phenomenon in three-dimensional tanks due to horizontal and roll excitations and investigated the prevention effect of different baffles on the sloshing. They reported that the horizontal baffle is more effective in decreasing the sloshing amplitude due to roll excitation compared to the horizontal excitation.

Liu *et al.* [14] established a CFD model to examine the thermal physical procedure and hydrodynamics of sloshing phenomenon in a cryogenic fuel storage tank. Liu *et al.* [15] offered a model to calculate the dynamic variation of the liquid-vapor interface numerically. They observed that the effect of the interface phase alteration develops increasingly with the increase of the sloshing amplitude for the free interface variation. Also, Liu *et al.* [16] studied the hydrodynamics of fluid sloshing in a cryogenic fuel storage tank for different natural frequencies. Their results specify that the natural frequency affects fluid sloshing.

In another study, Liu *et al.* [17] investigated the fluid sloshing thermo-mechanical behavior in a cryogenic fuel storage tank due to various acceleration of gravity levels. Also, Liu *et al.* [18] showed that the excitations of sloshing have great effects on the thermal procedure in cryogenic storage tanks.

Among baffles, the baffles with the ability to pass fluid can be interesting from different aspects. Nasar and Sannasiraj [19] investigated the performance of porous baffle arrangement on the sloshing phenomena in a barge-carrying liquid tank. Their results showed that the sway RAO is amplified at special frequencies due to augmented sloshing flow or phase synchronization between sloshing flow and sway response. Nasar *et al.* [20] studied the porous

baffle performance assessment on liquid sloshing dynamics in a barge-carrying liquid tank by the Smoothed Particle Hydrodynamics (SPH) method. It is learned that the effect of baffles on sway and roll replies is substantial. The SPH method, due to being Lagrangian, models free surface and two-phase flows more easily.

Shao *et al.* [21] proposed an improved SPH method for modeling liquid sloshing dynamics. It is seen that the SPH method can well cover physics associated with breaking and changing surfaces. Using the SPH method, Shamsoddini [22] investigated the horizontal and vertical baffle effects on the liquid sloshing phenomenon in a rectangular tank.

The results showed that by choosing the right size and mode of the baffles, fluctuations can be reduced by more than 40%. Using a 2D ISPH turbulent method, Shamsoddini and Abolpur [23] investigated the effects of baffles on shallow water sloshing in a rectangular tank. Their results show that the baffles have a critical role in the decrease of the sloshing fluctuations. A few studies have focused on numerical simulation of slashing phenomena with non-Newtonian fluid.

Among them, the work of Shamsoddini and Abolpour [24] can be mentioned, in which the phenomenon of sloshing with Bingham fluid is modeled by the SPH method. They showed that, in some cases, it is possible to reduce the fluctuations by 80%.

As seen in previous studies, the usual method to reduce the fluctuations of the sloshing phenomenon is the use of baffles. The usual baffles used are simple plate baffles. Previously, porous baffles were introduced as a type of permeable baffle to control the sloshing phenomenon. In the vast majority of these studies that have been conducted experimentally, the effects of hydrodynamic forces on baffles have not been investigated. In this work, in addition to the numerical investigation of the mesh baffle, the forces on the baffle are investigated. The authors' observations show that, in the case of a simple baffle, the hydrodynamic forces on the baffle are very significant. This force is transferred to the body, which can lead to problems and dangers. Therefore, its estimation, control, and reduction should be in order. So, in the present work, a mesh baffle is introduced and tested, which reduces the amount of hydrodynamic force to an acceptable level. To the best knowledge of the authors, no study has been done on the investigation of hydrodynamic forces on mesh baffles. The numerical analysis method is the Incompressible Smoothed Particle Hydrodynamics (ISPH) method, the solution details of which are described below.

2. Numerical procedure

Due to the complexities of the problem, the governing equations must simultaneously include the effects of turbulence and surface tension. The governing equations contain the equations of mass and momentum continuity as follows:

$$\nabla \cdot \boldsymbol{V} = 0 \tag{1}$$

$$\frac{D\boldsymbol{V}}{Dt} = -\frac{1}{\rho}\nabla p + \boldsymbol{g} + \frac{1}{\rho}\nabla, \boldsymbol{\tau} + \frac{1}{\rho}\boldsymbol{F_s} \tag{2}$$

where ρ, t, $\boldsymbol{V}$, p, $\boldsymbol{g}$ $\boldsymbol{\tau}$ are the density of each particle of the fluid, time, the velocity vector of the particle, pressure, gravity acceleration, and total shear stress tensor, respectively. The shear stress tensor is calculated by:

$$\boldsymbol{\tau} = \mu_e(\nabla \boldsymbol{u} + (\nabla \boldsymbol{u})^T) \tag{3}$$

$\boldsymbol{F_s}$ is the surface tension. It is estimated that the amount of this force is small compared to other forces and can be ignored, although it has been shown that it can be effective in some situations [25]. The SPH is used to solve the above equations. The discretization for $\nabla \boldsymbol{u}$ based on this method is:

$$\langle \nabla \boldsymbol{u} \rangle_i = \sum_j \forall_j (\boldsymbol{u}_j - \boldsymbol{u}_i)\, \boldsymbol{B}_i \cdot \nabla W_{ij} \tag{4}$$

where i and j are the counters of particles, $\boldsymbol{B}$ is the corrective tensor and W is the kernel function. For this function, the fifth-order Wendland kernel function is used (Wendland [26]) and the corrective tensor $\boldsymbol{B}$ is calculated by:

$$\boldsymbol{B}_i = -\left[\sum_j \forall_j r_{ij} \nabla W_{ij}\right]^{-1} \quad (5)$$

The model applied in the present study is the single-phase Newtonian fluid model. The flow is considered to be turbulence. Therefore, an effective viscosity is defined. The effective viscosity is predicted by

$$\mu_{e_i} = \mu_{f_i} + (\rho(c_s\delta)^2|\bar{\boldsymbol{S}}|)_i \quad (6)$$

where μ_{f_i} is the fluid viscosity, c_s equals 0.2, δ is the particle space, and $|\bar{\boldsymbol{S}}|$ is

$$|\bar{\boldsymbol{S}}| = \sqrt{2\boldsymbol{S}_{ij}:\boldsymbol{S}_{ij}}, \quad (7)$$

Then, $\langle\nabla,\boldsymbol{\tau}\rangle_i$ is calculated by:

$$\langle\nabla,\boldsymbol{\tau}\rangle_i = \sum_j 2\forall_j\left(\mu_{e_{ij}}\right)\frac{\boldsymbol{V}_i-\boldsymbol{V}_j}{r_{ij}}e_{ij},(\boldsymbol{B}_i,\nabla W_{ij}) \quad (8)$$

where $\mu_{e_{ij}} = (\mu_{e_i} + \mu_{e_j})/2$.
The last term of the momentum equation is the acceleration caused by the surface tension force. This force is equal to [27]:

$$\boldsymbol{F}_{s_i} = \sigma\boldsymbol{\kappa_i}\delta_{s_i} \quad (9)$$

in which, κ is equal to:

$$\boldsymbol{\kappa_i} = \sum_j \forall_j \boldsymbol{B}_i \cdot \nabla W_{ij} \cdot \left(\boldsymbol{n}_j - \boldsymbol{n}_i\right) \quad (10)$$

where $\boldsymbol{n}_i$ is the normal vector on the interface surface:

$$\boldsymbol{n}_i = \frac{\nabla\tilde{C}_i}{\left|\nabla\tilde{C}_i\right|} \quad (11)$$

where $\tilde{C}$ is the color function; the main phases are given the color number one, and the other is given the color number zero. In the single phase, there is no other phase. Therefore, it can be estimated by Ordoubadi *et al.* [28] method.

The last parameter in Eq. (9) is δ_{s_i}calculated by:

$$\delta_{s_i} = \left|\nabla\tilde{C}_i\right| \quad (12)$$

It is emphasized once again that although it was applied in the calculation code, the amount of this force in this study is insignificant compared to other forces. After calculating the shear stress and surface tension, the intermediate velocity is obtained according to the following equation:

$$\boldsymbol{V}_i^{*\,n+1} = \boldsymbol{V}_i^n + (\boldsymbol{g} + \frac{1}{\rho}\nabla,\boldsymbol{\tau} + \frac{1}{\rho}\boldsymbol{F_s})\Delta t \quad (13)$$

By the intermediate velocity, the Poisson pressure equation is discretized in the SPH form:

$$\sum_j 2\frac{\forall_j}{\rho_{ij}}\frac{P_i^{n+1}-P_j^n}{r_{ij}}e_{ij},\left(\boldsymbol{B}_i,\nabla W_{ij}\right) = \frac{\langle\nabla\cdot\boldsymbol{V}_i^{*\,n+1}\rangle}{\Delta t} \quad (14)$$

After computing the pressure, the ultimate velocity is considered as follows:

$$\boldsymbol{V}_i^{n+1} = \boldsymbol{V}_i^{*\,n+1} - \langle\frac{\nabla p}{\rho}\rangle_i^{n+1}\Delta t \quad (15)$$

Lastly, the position of the particle is rearranged by:

$$\boldsymbol{r}_i^{n+1} = \boldsymbol{r}_i^n + \boldsymbol{V}_i^{n+1}\Delta t \quad (16)$$

By dot multiplying the normal vector of surface in the momentum equation, the pressure on the wall is indicated:

$$\left(\frac{\nabla p}{\rho}\right)\cdot\boldsymbol{n}_w = -\frac{d\boldsymbol{V}_b}{dt}\cdot\boldsymbol{n}_w + \left(\nabla\cdot(\nu_e\nabla\boldsymbol{V})\right)\cdot\boldsymbol{n}_w + \boldsymbol{g},\boldsymbol{n_w} \quad (17)$$

where $\left(\frac{\nabla p}{\rho}\right)\cdot\boldsymbol{n}_w = \frac{1}{\rho}\frac{\partial p}{\partial n_w}$. The distance of dummy particles and wall is constant. Therefore, this equation can easily be discretized by the finite difference method. Among the weaknesses

of the SPH method, fracture, cluster alignment, and bonding of particles can be mentioned. A remedy to these unfavorable phenomena is particle shifting. One of the first studies of the particle shifting algorithm is the one done by Shadloo *et al.* [29]. In the present study, a shifting algorithm similar to that applied by Shamsoddini and Mofidi [30] is implemented.

For the single-phase flow, zero pressure is considered for the free surface particles. To indicate the free surface particles, a separate subroutine is implemented calculating the location vector divergence $\nabla \cdot \boldsymbol{r}$. This value is equal to 2.0 ($\nabla \cdot \boldsymbol{r} = 2$) for a two-dimensional problem. However, in the SPH calculations, the kernel space is not completely filled for the free surface particles. Therefore, this value becomes less than 2.0. Also, extra equivalent case is defined concurrently to certify the right selection of the free surface particle. For each particle, $\sum_j \forall_j W_{ij} = 1.0$. However, for the particle on the free surface, this value is less than one. So, in the present algorithm, a particle with $\sum_j \forall_j W_{ij}$ less than 0.85 is considered to be a free surface particle.

Another factor that needs to be considered in this research is the horizontal hydrodynamic force acting on the baffles, so in this part, the details of the relevant subroutine are discussed.

$$F_x = \int_A \left((\boldsymbol{\tau} - p\boldsymbol{I}) \cdot \boldsymbol{n}_x\right) dA, \qquad (18)$$

where n_x is unit vector of the x-direction, A is the baffle area.

This calculation algorithm is implemented in the form of a C^{++} calculation code.

3. Problem definition

In this section, first, the problem is described, then the effect of particle size on the accuracy of the calculations is discussed, and then the validation of the results for the base case is checked. An overview of the problem geometry is shown in Fig. 1. The problem consists of a tank with a rectangular cross-section, which has a width of 1.2 meters and a height of 0.6 meters, and about 60% of its height is filled with water.

4. Particle space and validation

In this section, the effect of particle space on the accuracy of calculations is investigated. For this purpose, four particle grids with different sizes are considered. In the initial arrangement, the particles are defined in a regular square arrangement where the distance between the adjacent particles in the x and y directions is equal to Δ. The tested values for Δ are equal to Δ=*W*/100, *W*/150, *W*/200, *W*/300, respectively. The results obtained from all four modes for the free surface at time *t*=15s for the case with no baffle are shown in Fig. 2. As can be seen, with the increase in the number of particles, more convergence is evident between the results. After checking the effects of the particle space, now it is time to check the accuracy of the calculations. For accuracy validation, the results of Godderidge *et al.* [31] are used.

The geometry of the problem is the same as the tank of the present work (Fig. 1) without considering the baffles.

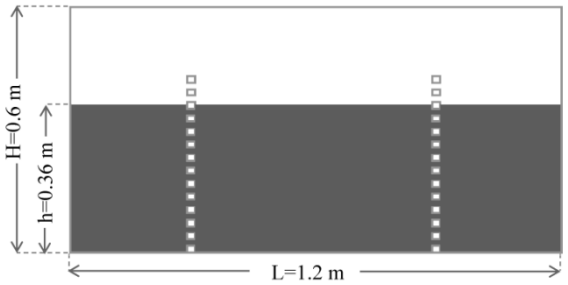

Fig. 1. The schematics, initial condition and geometrical sizes of the tank with grid baffles.

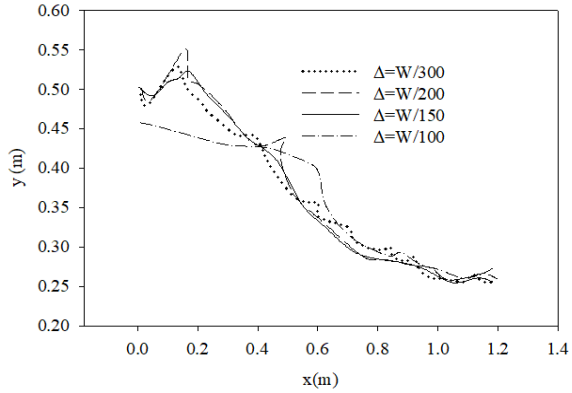

Fig. 2. Effects of particle space on the convergence of the results.

In simulating this problem, Godderidge *et al.* [31] presented a mesh-based numerical solution that agreed well with the experimental results. For this reason, these results have been used to validate the present particle work. The tank is stimulated by the formula:

$$x = Asin\left(\frac{2\pi t}{T}\right), \quad (19)$$

where A is the range of motion (A = 0.015m) and T is the period of motion (T = 1.404s). These quantities are applied based on the work of Godderidge *et al.* [31] so that a comparison with experimental results is possible. Fig. 3 shows the free surface profile obtained in the present study in comparison with those obtained by Godderidge *et al.* [31]. The obtained results show that the accuracy of the calculations is at an acceptable and reassuring level. Therefore, this computational algorithm is used to simulate the problem defined in Fig. 1.

5. Results and discussion

As mentioned, one of the ways to control the sloshing phenomenon is to use baffles. The authors' investigations show that simple baffles have a very high drag force. Therefore, in the present work, a sample of two-dimensional mesh baffles is tested, which both reduces the fluctuations caused by the sloshing phenomenon and reduces the drag force on the baffle.

In the first step, we examine the effect of both types of baffles on controlling the sloshing phenomenon.

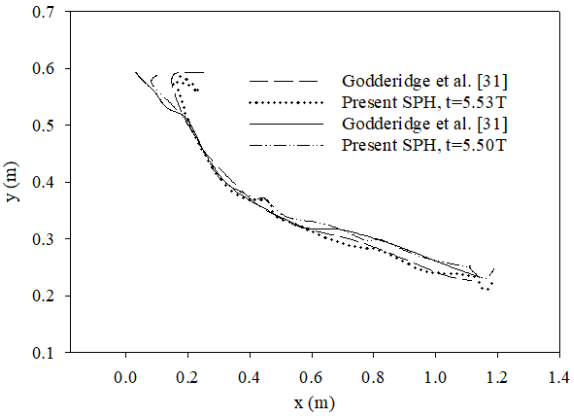

Fig. 3. Comparison of the free surface profile with the results of Godderidge *et al.* [31].

In Fig. 4, the pressure contours simultaneously show the changes of the cases in about one cycle (t/T=3.2 to t/T=4.27). Free surfaces of the flow are given for all three.

The dimensionless time shows the time (t) relative to the period of the forced movement of the tank (T). This non-dimensionalization helps to make periodic motion easier to understand and analyze. The motion and behavior of the fluid in each period will be more clearly traceable. As it is evident, in this case, the fluctuations are very intense, so that the fluctuations cover the entire surface of the vertical walls. But on the other hand, both the other modes, i.e. the mode with the simple baffle and the mode with the mesh baffle, dampen the oscillations well. In an experimental study, Nassar *et al.* [20] observed a significant reduction in free surface fluctuations using a porous baffle. However, one of the advantages of the numerical solution is that all the variables of the fluid field can be obtained at the same time. One of these variables, which is very important in analyzing the behavior of the sloshing phenomenon, is pressure. The no-baffle mode was previously investigated by Godderidge *et al.* [31]. They have extracted and analyzed the pressure changes at y/H=0.5. Therefore, first, the results of the present work are compared with their results, which are shown in Fig. 5. It shows that the simulation results in the no-baffle mode are completely consistent with the results of Godderidge *et al.* [31].

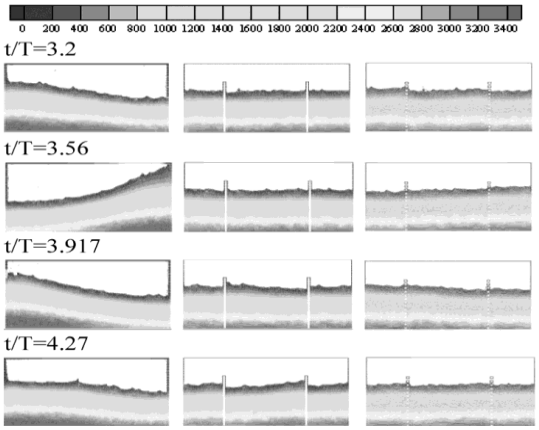

Fig. 4. Contour of pressure changes for the case without baffles (first column) compared to the cases with two simple (middle column) and mesh baffles (Last column).

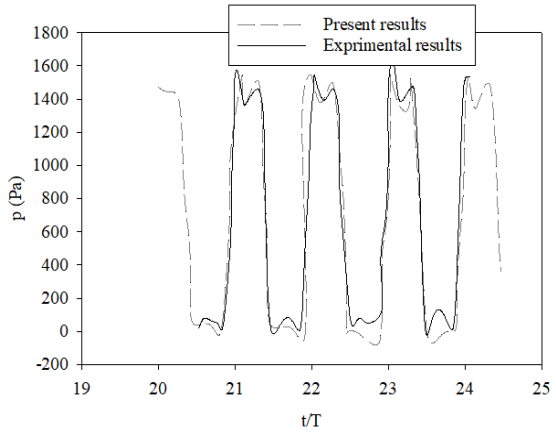

Fig. 5. Comparison of the present and experimental results [31]; pressure variation at y/H=0.5.

To have a suitable quantitative measure for the comparison, in Fig. 6, the average pressure changes with time on the right corner of the wall (y = 0) for all three cases are shown. As can be seen, the pressure changes are very large for the case where there is no baffle. In this case, the range of fluctuations is very high. In the other two modes (simple baffle mode and lattice baffle mode), the amplitude of oscillations is significantly reduced. However, the simple baffle model has reduced the fluctuations a bit more (the rate of reduction of simple baffle is 94% and the rate of reduction of mesh baffle is 85%.). The reduction of fluctuations is due to the fact that the kinetic energy of the fluid is used to overcome and pass the obstacles.

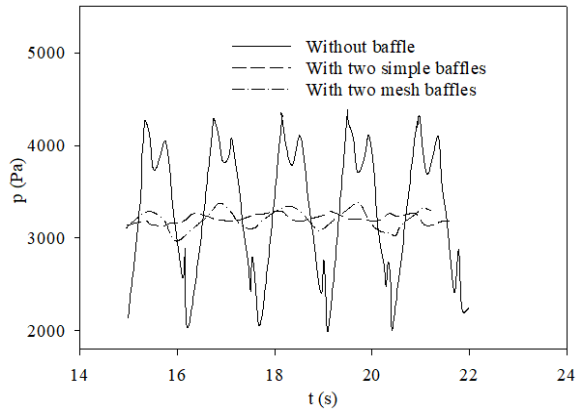

Fig. 6. Pressure variations on the base of the tank wall for the tank without baffle, with two simple baffles, and with two mesh baffles.

These conditions are also valid for the single baffle mode with a few more changes. Fig. 7 shows the pressure contours for the single-baffle mode in comparison with the no-baffle mode. The variations of the free surface are also well shown during almost one oscillation period. The results of this figure show that the existence of even one baffle, either in its simple form or in its mesh form, significantly reduces the fluctuations. In the next section, the variations of the horizontal force on each of the baffles are investigated.

5.1. Hydrodynamic force on each of the baffles

As mentioned earlier, baffles are primarily used to reduce hydrodynamic force fluctuations in the structure of liquid-carrying tanks. Since these baffles are usually installed on the inner wall of the tanks, the hydrodynamic forces on the baffles are finally transferred to the body. The tests conducted on the baffles resulted that these loads are very significant and sometimes lead to the breakage of the baffle from the connection to the tank. Therefore, the mesh baffle that, in addition to reducing pressure fluctuations, creates a less resistant hydrodynamic force is introduced. As seen in the previous section, both simple and mesh baffles effectively reduce pressure fluctuations on the tank wall.

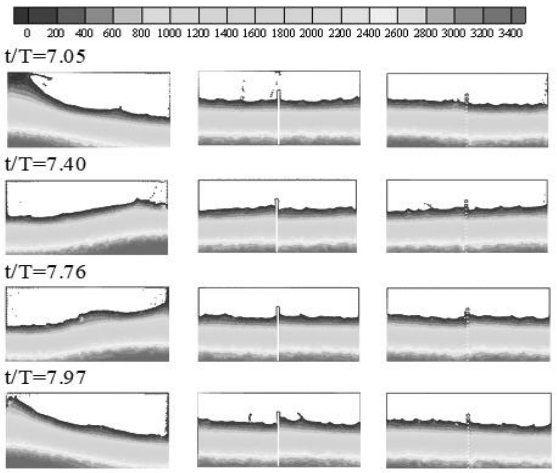

Fig. 7. Contour of pressure for the case without baffles (first column) compared to the cases with a simple baffle (second column) and mesh baffle (last column).

Now, in this section, the goal is to check the bearing force by the baffle itself. Therefore, in the following, the changes of the hydrodynamic force on the baffles in the case of single baffle and double baffle, for simple and mesh baffles are investigated.

In Fig. 8, the changes of the hydrodynamic force on the baffle in the single baffle mode are shown for both the simple baffle and mesh baffle modes. The hydrodynamic force for the case with mesh baffle is significantly reduced compared to the case with a simple baffle. This reduction is more than 80%.

In Fig. 9, the variations of the hydrodynamic force on each of the baffles are shown in the case where the tank has two simple or mesh baffles. Here too, the significant reduction of the hydrodynamic force on the mesh baffle compared to the simple baffle is quite evident.

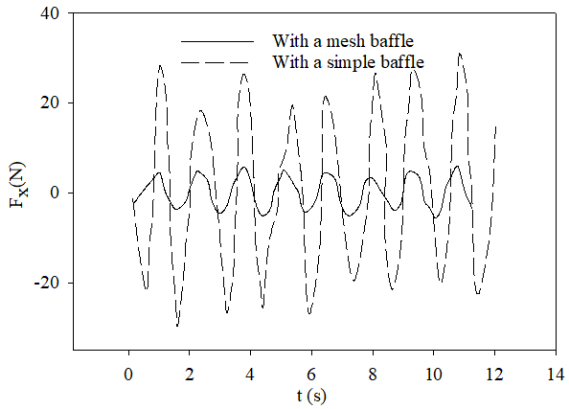

Fig. 8. Comparison of the hydrodynamic force on the baffle for the case with a simple or mesh baffle.

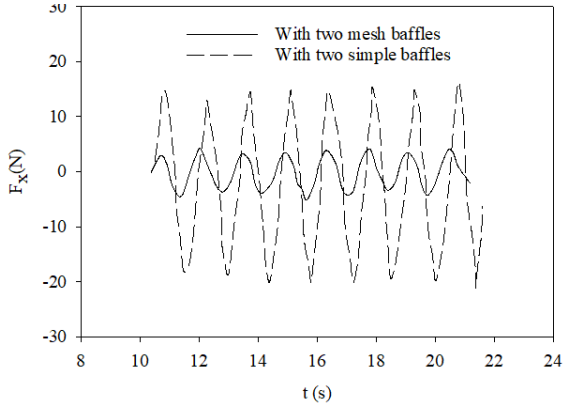

Fig. 9. Comparison of the hydrodynamic force on the baffles for the case with two baffles.

The comparison of Figs. 8 and 9 reveals that with the increase in the number of baffles, the hydrodynamic force is divided between the baffles (the forces in the double-baffle mode are about half of those in the single-baffle mode).

6. Conclusions

In the present work, to control the sloshing phenomenon, a mesh baffle was tested and investigated in comparison with the traditional simple baffle. An advanced SPH method was developed to simulate the tank with simple and mesh baffles and their results were compared. The results show that both baffles reduce the pressure fluctuations inside the tank well, although the simple baffle controls the pressure fluctuations a little better and more than the simple baffle (the rate of reduction of the simple baffle is 94% and the rate of reduction of mesh baffle is 85%.). The investigation of the results of the hydrodynamic forces on the baffles shows that the mesh baffle creates a much less resistant hydrodynamic force. On average, it can be said that a mesh baffle creates about 80% less resistive force compared to a simple baffle.

[1] V. J. Modi and S. R. Munshi, "An efficient liquid sloshing damper for vibration control" *J. Fluids Struct.*, Vol. 12, No 8, pp. 1055-1071, (1998).

[2] Y. Kim, B. W. Nam, D. W. Kim and Y. S. Kim, "Study on coupling effects of ship motion and sloshing", *Ocean Eng.*, Vol. 34, No. 16, pp. 2176-87, (2007).

[3] S. Brizzolara, L. Savio, M. Viviani, et al. "Comparison of experimental and numerical sloshing loads in partially filled tanks" *Ships Offshore Struct.*, Vol. 6, No. 1-2, pp. 15-43, (2011).

[4] M. A. Xue and P. Lin, "Numerical study of ring baffle effects on reducing violent liquid sloshing" *Comput. Fluids*, Vol. 52, pp.116-129. (2011).

[5] B. Molin and F. Remy. "Experimental and numerical study of the sloshing motion in a rectangular tank with a perforated

screen*" J. Fluids Struct.*, Vol. 43, pp. 463-480, (2013).

[6] N. Hosseinzadeh, M. K. Sangsari and H. T. Ferdosiyeh, "Shake table study of annular baffles in steel storage tanks as sloshing dependent variable dampers", *J. Loss. Prev. Process Ind*., Vol. 32, pp. 299-310, (2014).

[7] L. Lu, S. C. Jiang, M. Zhao and G. Q. Tang, "Two-dimensional viscous numerical simulation of liquid sloshing in rectangular tank with/without baffles and comparison with potential flow solutions", *Ocean Eng.*, Vol. 108, pp.662-677, (2015).

[8] I. H. Cho and M. H. Kim, "Effect of dual vertical porous baffles on sloshing reduction in a swaying rectangular tank" *Ocean Eng*., Vol. 126, pp. 364-373, (2016).

[9] M. A. Xue, J. Zheng, P. Lin and X. Yuan, "Experimental study on vertical baffles of different configurations in suppressing sloshing pressure", *Ocean Eng.*, Vol. 136, pp.178-189, (2017).

[10] S. Y. Kim, Y. Kim and J. Lee, "Comparison of sloshing-induced pressure in different scale tanks', *Ships Offshore Struct.*, Vol. 12, No. 2, pp. 244-261, (2017).

[11] W. Wang, Q. Zhang, Q. Ma and L. Ren, "Sloshing effects under longitudinal excitation in horizontal elliptical cylindrical containers with complex baffles" *J. Waterw. Port Coast. Ocean Eng.*, Vol. 144. No. 2, p. 04017044, (2018).

[12] J. H. Wang and S. L. Sun, "Study on liquid sloshing characteristics of a swaying rectangular tank with a rolling baffle", *J. Eng. Math.*, Vol. 119, No. 1, pp. 23-41, (2019).

[13] Y. Guan, C. Yang, P. Chen and L. Zhou. "Numerical investigation on the effect of baffles on liquid sloshing in 3D rectangular tanks based on nonlinear boundary element method", *Int. J. Nav. Archit. Ocean Eng*., Vol. 12, pp. 399-413, (2020).

[14] Z. Liu, H. Chen, Q. Chen and L. Chen, "Numerical Study on thermodynamic performance in a cryogenic fuel storage tank under external sloshing excitation", *Int. J. Aeronaut. Space Sci*., Vol. 22, No. 5, pp.1062-1074, (2021).

[15] Z. Liu, Y. Feng, J. Yan, Y. Li and L. Chen, "Dynamic variation of interface shape in a liquid oxygen tank under a sinusoidal sloshing excitation", *Ocean Eng*., Vol. 213, p.107637, 2020.

[16] Z. Liu, K. Yuan, Y. Liu, M. Andersson and Y. Li, "Fluid sloshing hydrodynamics in a cryogenic fuel storage tank under different order natural frequencies", *J. Energy Storage*, Vol. 52, pp. 104830, (2022).

[17] Z. Liu, K. Yuan, Y. Liu, Y. Qiu and G. Lei, "Fluid sloshing thermo-mechanical characteristic in a cryogenic fuel storage tank under different gravity acceleration levels", *Int. J. Hydrog. Energy*, Vol. 47, No. 59, pp.25007-25021, 2022.

[18] Z. Liu, Y. Feng, G. Lei and Y. Li, Thermal physical process in a liquid oxygen tank under different sloshing excitations. *Int. Commun. Heat Mass Transf*., Vol. 117, p.104771, (2020).

[19] T. Nasar and S. A. Sannasiraj, "Sloshing dynamics and performance of porous baffle arrangements in a barge carrying liquid tank", *Ocean Eng*., Vol. 183, pp. 24-39, (2019).

[20] T. Nasar, S. A. Sannasiraj and V. Sundar, "Performance assessment of porous baffleon liquid sloshing dynamics in a barge carrying liquid tank", *Ships Offshore Struct*., Vol. 16, No. 7, pp. 773-786. (2021).

[21] J. R. Shao, H. Q. Li, G. R. Liu and M. B. Liu. "An improved SPH method for modeling liquid sloshing dynamics", *Comput. Struct*., Vol. 100, pp. 18-26, (2012).

[22] R. Shamsoddini, "Numerical investigation of vertical and horizontal baffle effects on liquid sloshing in a rectangular tank using an improved incompressible smoothed particle hydrodynamics method", *J. Comput., Appl. Res. Mech. Eng.*, Vol. 8, No. 2, pp.175-186, (2019).

[23] R. Shamsoddini and B. Abolpur, "Investigation of the effects of baffles on the shallow water sloshing in a rectangular tank using a 2D turbulent ISPH method"

China Ocean Eng., Vol. 33, pp. 94-102, (2019).
[24] R. Shamsoddini and B. Abolpour, "Bingham fluid sloshing phenomenon modelling and investigating in a rectangular tank using SPH method", *Ships Offshore Struct.*, Vol. 16, No. 5, pp. 557-566, (2021).
[25] B. Meziani, and O. Ouerdia, "Capillary effect on the sloshing of a fluid in a rectangular tank submitted to sinusoidal vertical dynamical excitation". *J. Hydrodynamics B*, Vol. 26, No. 2, pp. 326-338, (2021).
[26] H. Wendland, "Piecewise polynomial, positive definite and compactly supported radial functions of minimal degree" *Adv. Comput. Math.*, Vol. 4, pp. 389-396. (1995).
[27] M. S. Shadloo, A. Zainali and M. Yildiz, "Simulation of single mode Rayleigh–Taylor instability by SPH method", *Comput. Mech.*, Vol. 51, pp. 699-715, (2013).
[28] M. Ordoubadi, M. Yaghoubi and F. Yeganehdoust. "Surface tension simulation of free surface flows using smoothed particle hydrodynamics", *Scientia Iranica*, Vol. 24, No. 4, pp. 2019-2033, (2017).
[29] M. S. Shadloo, A. Zainali, S. H. Sadek and M. Yildiz, "Improved incompressible smoothed particle hydrodynamics method for simulating flow around bluff bodies" *Comput. Methods Appl. Mech. Eng.*, Vol. 200, No. 9-12, 1008-1020, (2011).
[30] R. Shamsoddini and M. Mofidi, "ISPH modeling and investigation of the effect of viscosity variations on the fluids mixing in a micro-channel due to oscillation of a circular cylinder" *J. Taiwan Inst. Chem. Eng.*, Vol. 118, pp.78-86, (2021).
[31] B. Godderidge, S. Turnock, M. Tan and C. Earl, "An investigation of multiphase CFD modelling of a lateral sloshing tank" *Comput. Fluids*, Vol. 38, No. 2, pp. 183-193, (2009).

How to cite this paper:

R. Shamsoddini and B. Abolpour, "Comparison of the performance of mesh and simple baffles in controlling the sloshing phenomenon based on the SPH simulation,", *J. Comput. Appl. Res. Mech. Eng.*, Vol. 13, No. 2, pp. 219-228, (2024).

DOI: 10.22061/JCARME.2024.10109.2353

URL: https://jcarme.sru.ac.ir/?_action=showPDF&article=2054